Supplementary Information

Photodissociation dynamics of fulvenallene and the fulvenallenyl radical at 248 and 193 nm

Isaac A. Ramphal,[†,‡] Mark Shapero, [†,‡] Courtney Haibach-Morris, [‡] Daniel M. Neumark*,[†,‡]
[†]Chemical Sciences Division, Lawrence Berkeley National Laboratory, Berkeley, California 94720, United States
[‡]Department of Chemistry, University of California, Berkeley, California 94720, United States

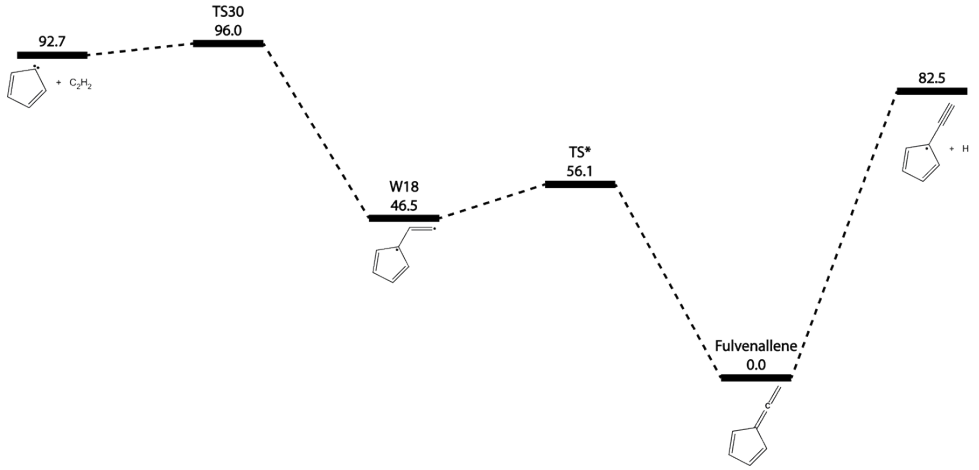

Figure S1. A simplified C_7H_6 potential energy diagram showing the production of C_7H_5 + H and C_5H_4 + C_2H_2 according predictions by Polino and Cavalotti.[1] The molecular naming scheme of the original work is used here. TS* separates the singlet and triplet surfaces.

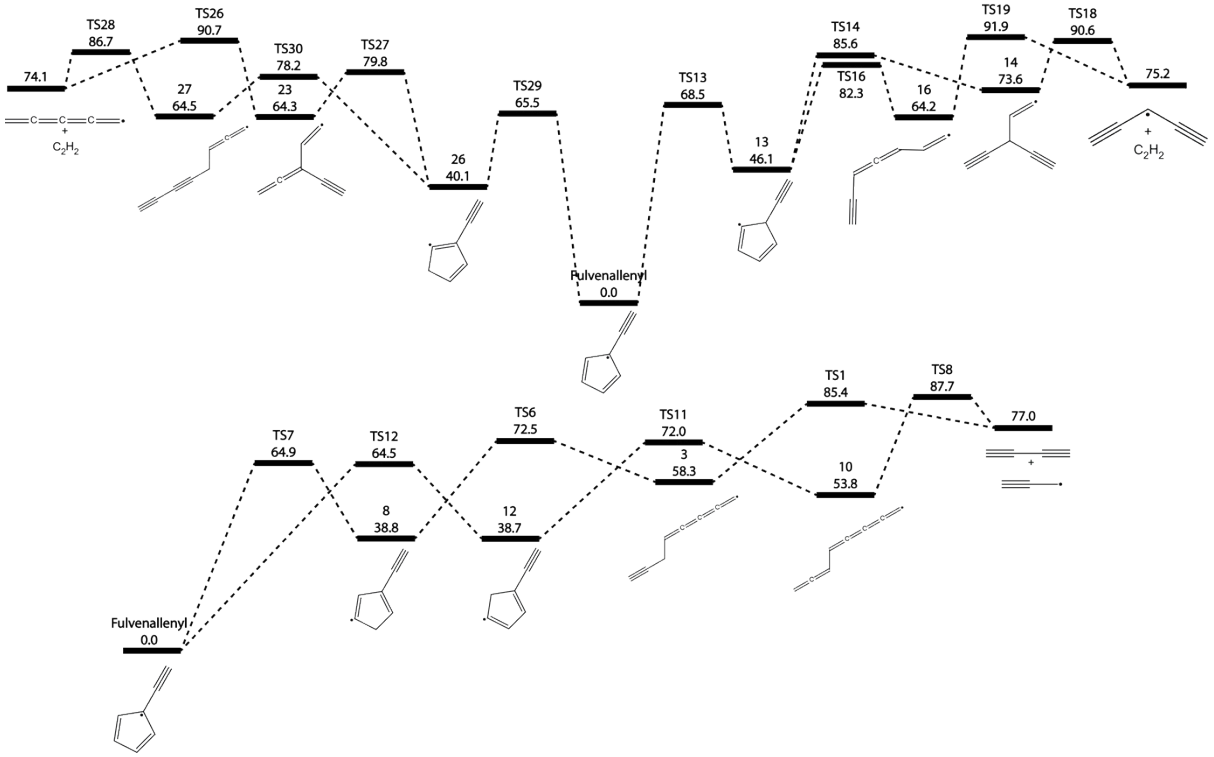

Figure S2. A simplified C_7H_5 potential energy diagram showing the production of C_5H_3 + C_2H_2 (top) and C_4H_2 + C_3H_3 (bottom) according to predictions by da Silva and Trevitt.[2] The molecular naming scheme of the original work is used here. The RRKM calculations done in this study use the full potential energy surface from the original work.

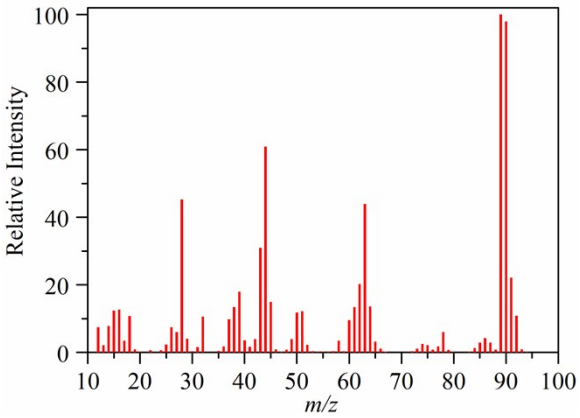

Figure S3. Mass spectrum of fulvenallene in the standardized format used by NIST, collected with 80 eV electron energy and normalized to the *m/z* = 89 signal intensity. There is likely an appreciable contribution to the signal at *m/z* = 28 and 14 due to high N_2 background in the detector.

Table S1. Oscillator strengths and orbital symmetries for vertical transitions of fulvenallene and fulvenallenyl in the vicinity of 248 nm and 193 nm, calculated using time-dependent DFT at the B3LYP 6-311G++(d,p) level.

	Fulvenallene		**Fulvenallenyl**	
Absorption Energy	241 nm	197 nm	254 nm	191 nm
Oscillator Strength	0.436	0.024	0.219	0.007
Transition Symmetry	$4\ {}^{1}\tilde{A}_1 \leftarrow X\ {}^{1}\tilde{A}_1$	$11\ {}^{1}\tilde{B}_1 \leftarrow X\ {}^{1}\tilde{A}_1$	$5\ {}^{2}\tilde{A}_1 \leftarrow X\ {}^{2}\tilde{B}_1$	$15\ {}^{2}\tilde{A}_1 \leftarrow X\ {}^{2}\tilde{B}_1$

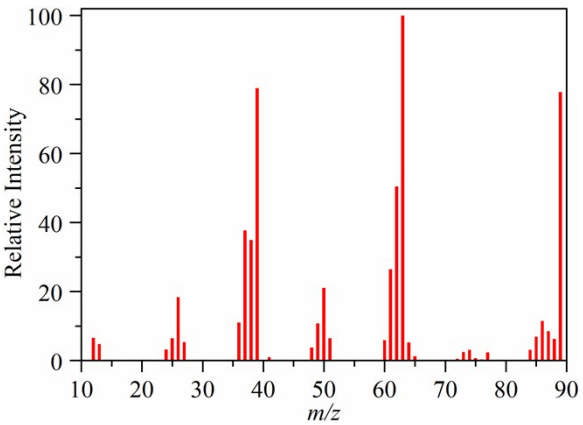

Figure S4. Mass spectrum of the fulvenallenyl radical in the standardized format used by NIST, collected with 80 eV electron energy and normalized to the *m/z* = 63 signal intensity. Values of *m/z* < 12 were not measured. High detector background at *m/z* = 28 and 14 from N_2^+ and N_2^{2+}/N^+ respectively and at *m/z* = 40 from Ar^+ preclude measurement of these signals. This spectrum was collected by measuring TOF spectra with *m/z* of all possible combinations of up to seven C atoms and five H atoms at Θ_{LAB} = 5°. The signal for each spectrum was normalized by the *m/z* = 89 signal at 5° that was continually remeasured throughout the experiment.

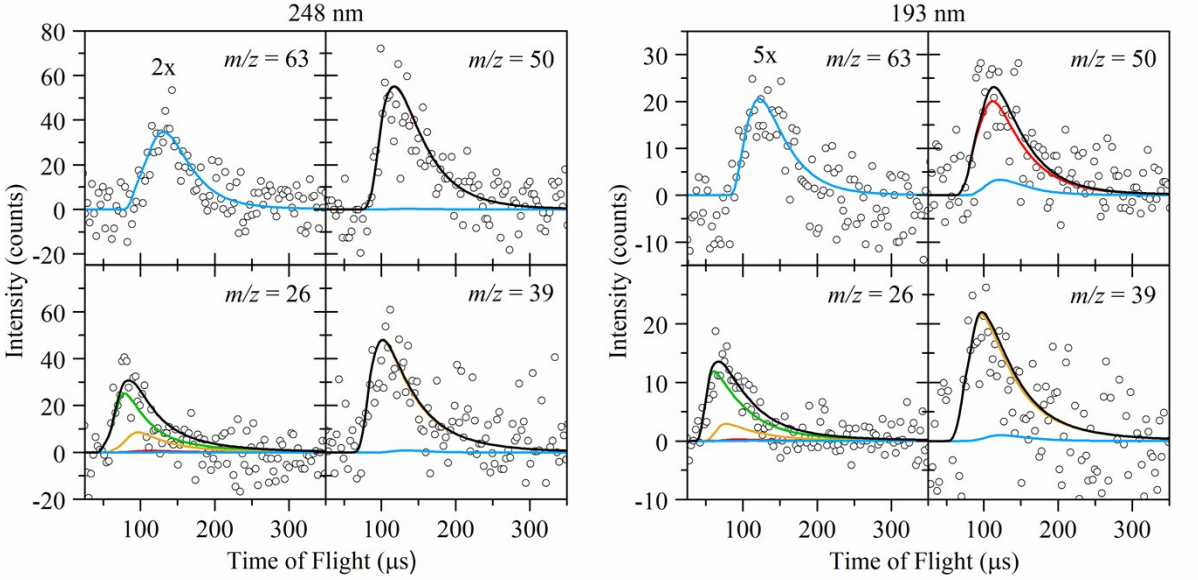

Figure S5. TOF spectra for m/z = 63 (top left panels), m/z = 26 (bottom left panels), m/z = 50 (top right panels) and m/z = 39 (bottom right panels) at Θ_{LAB} = 30° ($\Phi_{248\,nm} = 420\ mJ\ cm^{-2}$, $\Phi_{193\,nm} = 300\ mJ\ cm^{-2}$). The blue ($m/z$ = 63) and green (m/z = 26) simulations are generated using the $P(E_T)$ in Figures 9a and 9c, while the red (m/z = 50) and yellow (m/z = 39) simulations are generated using the $P(E_T)$ in Figures 9b and 9d. For TOF spectra with multiple features, the total simulation is shown in black.

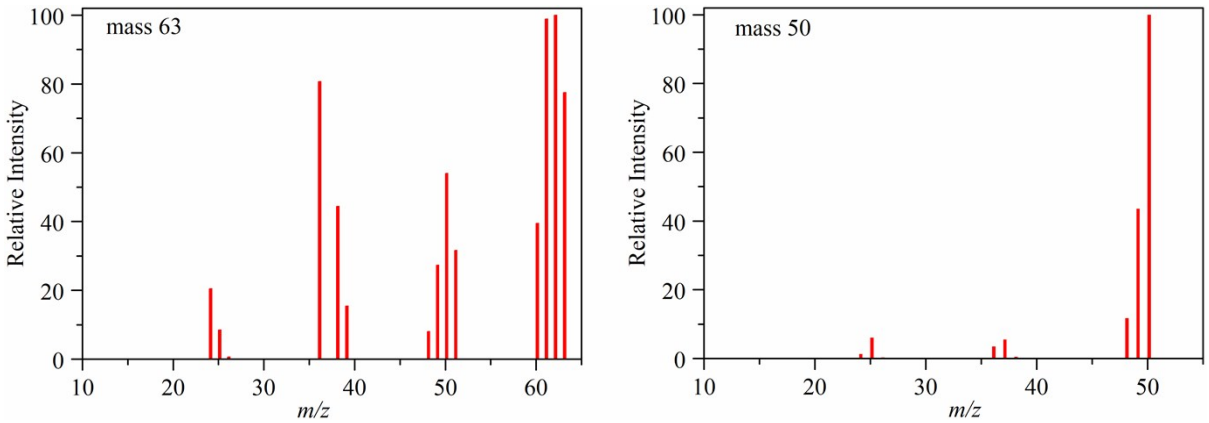

Figure S6. Mass spectrum of the mass 63 (left) and 50 (right) photofragments in the standardized format used by NIST, collected with 80 eV electron energy and normalized to the m/z = 62 and 50 signal intensities respectively. Values of m/z < 12 were not measured. High detector background at m/z = 14 from N_2^{2+}/N^+ precludes measurement of these signals. The same technique described in Fig. S4 was used to collect these spectra, with measurements taken at Θ_{LAB} = 10°. This angle is beyond the fulvenallene H-atom loss Newton sphere so that any contributions from this channel to the TOF signal are removed.

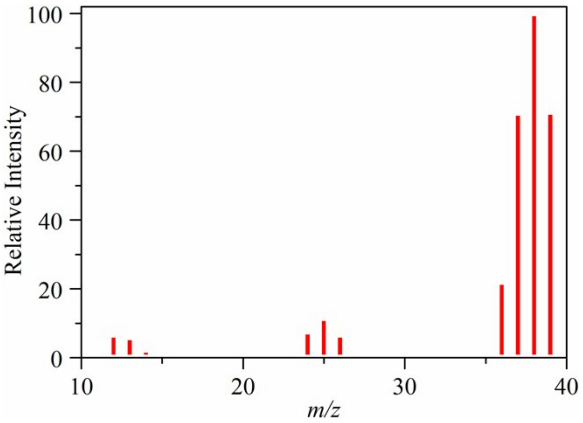

Figure S7. Mass spectrum of the propargyl radical in the standardized format used by NIST, collected with 180 eV electron energy and normalized to the *m/z* = 38 signal intensity. Values of *m/z* < 12 were not measured. The same technique described in Fig. S4 was used to collect this spectrum. These previously unpublished data were collected during studies of allene photodissociation, for which loss of an H atom to form the propargyl radical is the dominant channel.[3]

Consecutive Photodissociation Processes

Figure 5 shows that photofragments with *m/z* < 64 have a different laser fluence dependence than the *m/z* = 89 ($C_7H_5^+$) feature produced by fulvenallene H-atom loss. This behavior is suggestive of the presence of secondary photodissociation. For an experiment in which primary photoproducts undergo secondary photodissociation in the consecutive reaction scheme

$$A \xrightarrow{h\nu} B \xrightarrow{h\nu} C$$

where A is fulvenallene, B is fulvenallenyl, and C is the sum of secondary dissociation channel products, the rate equations governing concentration changes in each species are

$$\frac{dA(t)}{dt} = -\frac{\sigma_A \phi(t)}{h\nu} A(t) \tag{1a}$$

$$\frac{dB(t)}{dt} = \frac{\sigma_A \phi(t)}{h\nu} A(t) - \frac{\sigma_B \phi(t)}{h\nu} B(t) \tag{1b}$$

$$\frac{dC(t)}{dt} = \frac{\sigma_B \phi(t)}{h\nu} B(t) \tag{1c}.$$

In 1a-c, σ_A and σ_B are the absorption cross-sections of fulvenallene and the fulvenallenyl radical respectively and $\phi(t)$ is the intensity of the laser pulse as a function of time. We assume dissociation is instantaneous. Integrating $\phi(t)$ over the duration of the laser pulse gives the total intensity Φ contained in the pulse. Solving for the concentrations of A, B, and C after the laser pulse has finished gives

$$A = A_o \, e^{-\sigma_A \Phi / h\nu} \tag{2a}$$

$$B = \frac{\sigma_A}{\sigma_B - \sigma_A} A_o \left(e^{-\sigma_A \Phi / h\nu} - e^{-\sigma_B \Phi / h\nu} \right) \tag{2b}$$

$$C = A_o \left\{ \frac{\sigma_B}{\sigma_B - \sigma_A} \left(1 - e^{-\sigma_A \Phi / h\nu} \right) - \frac{\sigma_A}{\sigma_B - \sigma_A} \left(1 - e^{-\sigma_B \Phi / h\nu} \right) \right\} \tag{2c}.$$

Given the results of the TD-DFT calculations (Table S1), we expect that the ratio of calculated oscillator strengths for electronic excitations compares approximately to the ratio of absorption cross-sections such that for 248 nm excitation $\frac{\sigma_A}{\sigma_B} \approx 2$ and for 193 nm excitation $\frac{\sigma_A}{\sigma_B} \approx 3$.[4] Therefore, the only free parameter in these functions is σ_A, the absorption cross-section of fulvenallene. From the TD-DFT results we also expect that $\frac{\sigma_{A,\,248\,nm}}{\sigma_{A,\,193\,nm}} \approx 18$.

The laser fluence dependence of the *m/z* = 89 ($C_7H_5^+$) and *m/z* = 50 ($C_4H_2^+$) TOF features is shown in Figure S8. The *m/z* = 50 ($C_4H_2^+$) data were collected beyond the fulvenallene H-loss Newton circle, and so contain no DI signal from fulvenallenyl. The expected linear dependence of signal intensity for a single-photon absorption process is not observed, nor is the quadratic dependence that should arise were fulvenallene to absorb two photons. Best fits of Equation 2 to select data, obtained by varying σ_A, are shown in Figure S8, with the experimentally derived cross-sections presented in Table S2. The fitting routine involves a global fit to the *m/z* = 89 ($C_7H_5^+$) and *m/z* = 50 ($C_4H_2^+$) data, as well as similar data for *m/z* = 62 ($C_5H_2^+$, not shown) at each wavelength.

The consecutive two-photon model matches well with the observed laser fluence dependence. Fitting the photofragment signal dependence on incident laser fluence with this model produced good fits at each wavelength for both species having absorption cross-sections in the range of 10^{-20}-10^{-18} cm^2 per molecule (Table S2). For fulvenallene, $\sigma_{248\,nm} = (3.1 \pm 0.1) \times 10^{-18}\,cm^2$ compares quite well with a previously reported experimental value of $\sigma_{266\,nm} = (3.4 \pm 0.5) \times 10^{-18}\,cm^2$ for a similar energy absorption.[5]

A competing, concerted two-photon process whereby fulvenallene absorbed two ultraviolet photons and dissociated to produce the fulvenallenyl radical, which then further dissociates, is conceivable. Our fulvenallene H-loss P(E_T)'s do not match well with two-photon prior distributions at 248 nm or at 193 nm. If this process were to occur the laser fluence dependence should be quadratic for the *m/z* = 63, 50, 39 and 26 photofragments, contrary to what is observed experimentally.

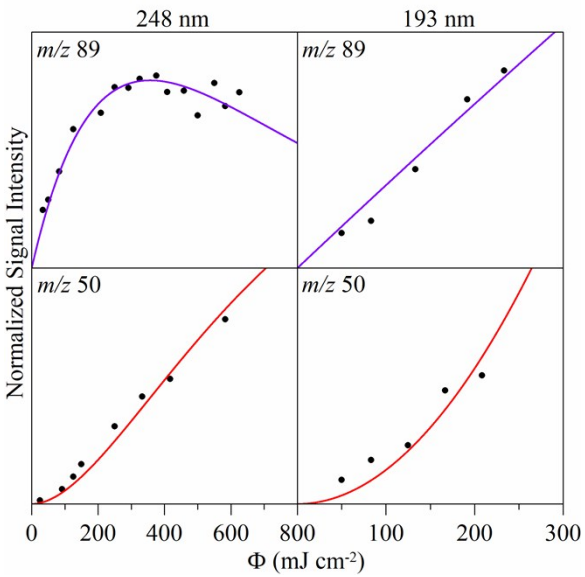

Figure S8. Laser fluence dependence of primary photofragment *m/z* = 89 (top) and secondary photofragment *m/z* = 50 (bottom) upon photoexcitation of fulvenallene at 248 nm (left) and 193 nm (right). Fits to the data are made using Equations 2b and 2c for primary and secondary photofragment concentration as a function of laser fluence.

Table S2. Absorption cross-sections of fulvenallene and fulvenallenyl determined by fitting the laser power dependence of primary and secondary photoproducts.

λ (nm)	**σ (× 10^{-19} cm^2 per molecule)**	
	Fulvenallene	*Fulvenallenyl*
248	31 ± 1	16.0 ± 0.5
193	1.70 ± 0.05	0.52 ± 0.02

References

1. D. Polino and C. Cavallotti, *J. Phys. Chem. A*, 2011, **115**, 10281-10289.

2. G. da Silva and A. J. Trevitt, *Phys. Chem. Chem. Phys.*, 2011, **13**, 8940-8952.
3. J. C. Robinson, N. E. Sveum, S. J. Goncher and D. M. Neumark, *Mol. Phys.*, 2005, **103**, 1765-1783.
4. R. C. Hilborn, *Am. J. Phys.*, 1982, **50**, 982-986.
5. M. A. Oehlschlaeger, D. F. Davidson and R. K. Hanson, *J. Phys. Chem. A*, 2006, **110**, 6649-6653.